RSC Advances

PAPER

View Article Online
View Journal | View Issue

Cite this: *RSC Adv.*, 2015, **5**, 19944

Synthesis and biological evaluation of non-glucose glycoconjugated *N*-hydroxyindole class LDH inhibitors as anticancer agents†

Valeria Di Bussolo,[a] Emilia C. Calvaresi,‡[b] Carlotta Granchi,[a] Linda Del Bino,[a] Ileana Frau,[a] Maria Chiara Dasso Lang,§[a] Tiziano Tuccinardi,[a] Marco Macchia,[a] Adriano Martinelli,[a] Paul J. Hergenrother*[b] and Filippo Minutolo*[a]

Received 16th January 2015
Accepted 10th February 2015

DOI: 10.1039/c5ra00946d

www.rsc.org/advances

Inhibitors of human lactate dehydrogenase A (LDH-A) are promising therapeutic agents against cancer. The development of LDH-A inhibitors that possess cellular activities has so far proved to be particularly challenging, since the enzyme's active site is narrow and highly polar. In the recent past, we were able to develop a glucose-conjugated *N*-hydroxyindole-based LDH-A inhibitor designed to exploit the sugar avidity expressed by cancer cells (the Warburg effect). Herein we describe a structural modulation of the sugar moiety of this class of inhibitors, with the insertion of α-D-mannose, β-D-gulose, or β-*N*-acetyl-D-glucosamine portions in their structures. Their stereospecific chemical synthesis, which involves a substrate-dependent stereospecific glycosylation step, and their biological activity in reducing lactate production and proliferation in cancer cells are reported. Interestingly, the α-D-mannose conjugate displayed the best properties in the cellular assays, demonstrating an efficient antiglycolytic and antiproliferative activity in cancer cells.

Introduction

Tumors generally follow unusual metabolic pathways to obtain the energy and anabolites required for their persistent growth. Growing cancer cells rewire their metabolism to meet their bioenergetic and biosynthetic needs for rapid proliferation by increasing their consumption of glucose and glutamine, enhancing glycolysis, and increasing the excretion of lactate. In particular, glycolysis, rather than oxidative phosphorylation (OXPHOS), is predominantly used even in the presence of oxygen, as described by the well-known "Warburg effect".[1,2] In fact, in normal cells, most of the pyruvate produced by glycolysis goes into the tricarboxylic acid (TCA) cycle and is eventually oxidized to CO_2 *via* OXPHOS. On the contrary, tumor cells mostly convert pyruvate to lactate anaerobically. Several prospective drugs have been developed to take advantage of this peculiar metabolism occurring in cancer by acting as antiglycolytic agents, as reviewed recently.[3,4]

Lactate dehydrogenase (LDH), the enzyme that catalyzes the interconversion of pyruvate and lactate, establishes a key checkpoint for the switch from aerobic to anaerobic glycolysis. LDH is a tetrameric enzyme that may exist in five isoforms (*h*LDH1-5), which results from the possible combinations of the two subunits: LDH-A and LDH-B. Subunit LDH-A (and, consequently, its tetrameric functional form *h*LDH5 or LDH-A_4) is very frequently found to be overexpressed in invasive cancer; its genetic silencing has been shown to reduce proliferation and invasiveness of tumor cells, especially under hypoxic conditions.[5] The validity of LDH-A as an anticancer target is further strengthened by the fact that individuals homozygous for LDH-A deficiency do not show any particular clinical symptoms, except for myoglobinuria upon intense physical exertion.[6] Therefore, several recent research efforts have been dedicated to the development of new LDH-A inhibitors with therapeutic potential as anticancer drugs, although problems related to poor cellular activities of these inhibitors have been often reported.[7,8]

The high rate of glycolysis in cancer cells is associated with a striking glucose avidity. This feature has been exploited by glycoconjugation of anticancer drugs, in order to improve their targeting to tumor cells *versus* normal tissues.[9] We have previously developed a novel class of *N*-hydroxyindole (NHI)-based LDH-A inhibitors,[10,11] and we recently reported that glucoconjugated NHIs, in particular NHI-Glc-2 (**1**, Fig. 1), showed a

[a]*Dipartimento di Farmacia, Università di Pisa, Via Bonanno 33, 56126 Pisa, Italy. E-mail: filippo.minutolo@farm.unipi.it*

[b]*Department of Chemistry, University of Illinois, 600 S. Mathews Avenue, Urbana, IL 61801, USA. E-mail: hergenro@illinois.edu*

† Electronic supplementary information (ESI) available: NMR spectra of **2–4**, **9**, **12–14**, **16–19** and **21**; HRMS of **2–4**; calibration curves of **1–3**. See DOI: 10.1039/c5ra00946d

‡ Present address: College of Medicine, University of Illinois, 506 S. Mathews Avenue, Urbana, IL 61801, USA.

§ Present address: Dipartimento di Biotecnologia, Chimica e Farmacia, Università degli Studi di Siena, *via* Aldo Moro 2, 53019 Siena, Italy.

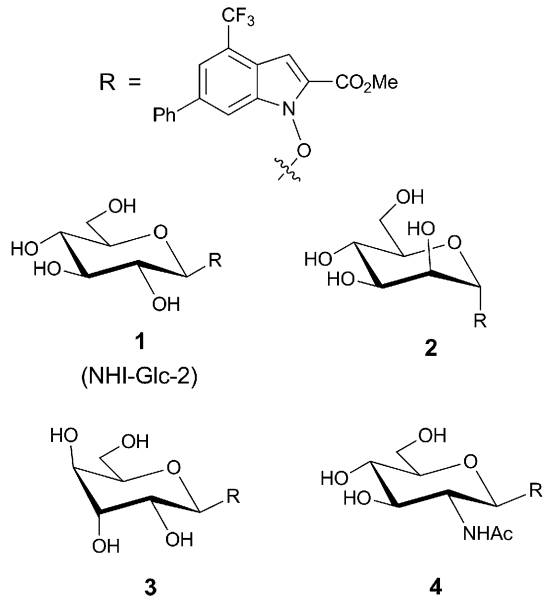

Fig. 1 Chemical structures of the NHI-glycoconjugates: β-D-Glc-(**1**), α-D-Man-(**2**), β-D-Gul-(**3**), and β-D-Glc(NAc)-(**4**) NHIs.

remarkably improved potency in reducing the cellular production of lactic acid in cancer cells.[12] Anticancer glycoconjugates are not limited to D-glucose; other sugar and aminosugar moieties have been previously introduced in anticancer agents with improved selectivity. This is due to the fact that glucose transporters overexpressed by tumor tissues, such as GLUT1, are able to transport a number of sugar substrates besides glucose.[9] Therefore, the ability of glucose analogues, such as α-manno-**2** and β-gulo-conjugate **3**, to be efficiently taken up by cancer cells, results in an attractive strategy of extending our "dual targeting" of the Warburg effect.[12] to a wider class of sugar conjugates. Compound **2** is a conjugate of D-mannose, a C2 epimer of D-glucose; D-mannose is found at concentrations of around 50 μM in human serum, and it is primarily used in the glycosylation of proteins (specifically, mannose-6-phosphate is a localization tag applied to proteins destined for lysosomal import). Mannose is known to be transported into mammalian cells primarily by mannose-specific transporters normally expressed in intestinal cells; however, it has also been reported to be a good substrate for GLUT1 (ref. 13) with a 13-fold reduction of its affinity for this transporter ($K_m = 20$ mM), when compared to that of glucose ($K_m = 1.5$ mM).[14] Compound **3** contains D-gulose, which is a stereoisomer of glucose differing in stereochemistry at the C3 and C4 positions; it is used by some archaea but it is not known to be found in human serum or used in human metabolism. So far, the ability of D-gulose to be transported by GLUTs has not been reported. In addition, since cancer cells have been found to utilize *O*-GlcN-acylation as a post-translational modification,[15,16] we also synthesized compound **4**, in which the NHI pharmacophoric unit is conjugated with GlcNAc.

Herein, we describe the application of our originally-developed glycosylation protocols to the synthesis of glycoconjugates **2–4** (Fig. 1) and their biological evaluations as prospective anticancer agents interfering with the cellular production of lactic acid.

Results and discussion

Synthesis of the glycoconjugates

Recently, we reported a new glycosylation process, using glycal derived vinyl epoxides **6α** and **6β** as new glycosyl donors (Scheme 1). These systems, in the presence of alcohols or alkyl lithium reagents as nucleophiles, afford only 6-*O*-benzyl-protected *O*- and *C*-glycosides with the same configuration of the starting epoxide, in an uncatalyzed substrate-dependent stereospecific process.[17–19] The driving force of this regio- and stereoselective 1,4-addition process is the occurrence of a coordination between the nucleophile and the oxirane oxygen in the form of hydrogen bond, in the case of *O*-nucleophile, or through the metal lithium cation, in the case of alkyl lithium reagents. Vinyl epoxides **6α** and **6β** cannot be isolated, because they are unstable and, therefore, they must be prepared only *in situ* by cyclization under basic conditions with *t*-BuOK of their ultimate precursor, the corresponding *trans*-hydroxymesylates **5** and **7**.

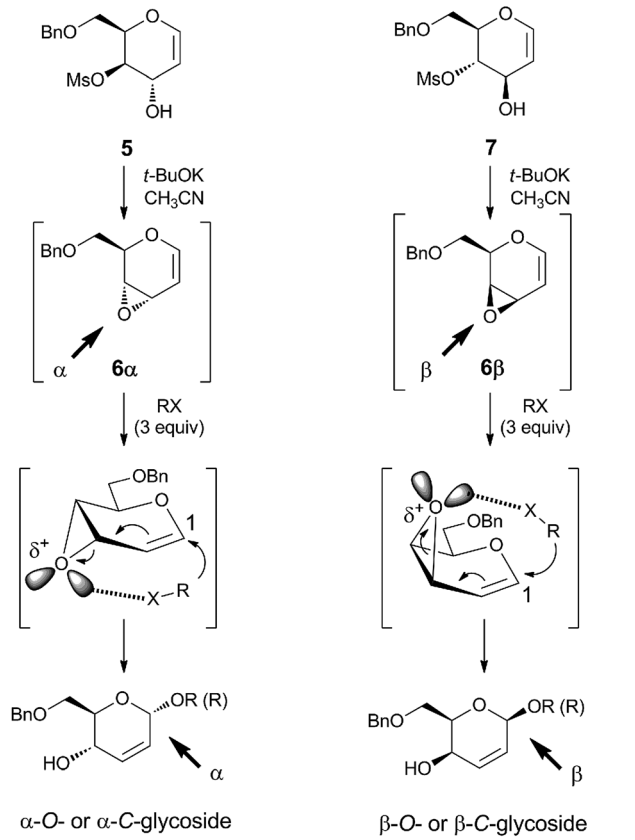

Scheme 1 Substrate-dependent stereospecific glycosylation: reaction conditions and mechanism of the stereochemical outcome [*O*-nucleophiles (alcohols), X = OH; *C*-nucleophiles (lithium alkyls), X = Li; R = Me, Et, i-Pr, *t*-Bu, Ph, monosaccharides].

In the synthesis of glycoconjugates **2** and **3**, due to the instability the N–O single bond under the reductive conditions utilized for the final removal of the benzyl protective group which was present in our original methodology (see **6α** and **6β**, Scheme 1), we decided to use synthetic intermediates in which the primary hydroxy functionality is protected as a tetrahydropyranyl ether (–OTHP), a protective group which can be easily removed by acid hydrolysis. The key intermediates are represented by THP-protected hydroxymesylate **8**, which was synthesized in six steps starting from tri-*O*-acetyl-D-glucal as previously reported[20] and **9**, which was instead specifically synthesized from **8** (Scheme 2). The conversion of **8** to **9** started with a cyclization with *t*-BuOK in CH_3CN, leading to the *in situ* formation of epoxide **10β**, which was followed by a ring opening reaction with a non-coordinating hydroxy ion equivalent, such as Me_3SiO^- present in $Bu_4N^+Me_3SiO^-$, a salt prepared by addition of potassium trimethyl silanolate (Me_3SiOK) to a solution of tetrabutyl ammonium bromide (TBAB) in THF.[19] In this way, after exposure to water, a clean 1,2-addition process is obtained, affording the desired *trans* diol **12**, which was treated with TBSCl to give the mono allyl C(3)-*O*-TBS derivative **13**. Subsequent mesylation of **13** at C(4) produced the all-protected glycal derivative **14**, which was finally deprotected with TBAF/THF to give *trans* hydroxymesylate **9**.

The synthesis of β-gulo-derivative **3** started from *trans*-hydroxymesylate **8** (Scheme 3), with the *in situ* formation of vinyl epoxide **10β** by cyclization with *t*-BuOK in CH_3CN. This reactive intermediate was not isolated. It was immediately treated with the NHI-based glycosyl acceptor **15** (NHI-2, a LDH-A inhibitor previously reported by us[11]) to give, after only 30 minutes at room temperature, the glycosylation product **16** with complete 1,4-regio- and β-stereoselectivity. Functionalization of the double bond present in **16** by OsO_4/NMO protocol afforded the corresponding *syn*-dihydroxylated product **18**, in accordance with a complete sterically-favored α-facial stereoselective electrophilic addition (70% yield). The deprotection of the C(6)-OTHP functionality of **18** by using catalytic PPTS in absolute EtOH under controlled temperature at 40 °C for 46 h, afforded the desired β-*O*-D-gulo-conjugate **3** in good yield after recrystallization (75% yield). A similar protocol was utilized for the preparation of the α-manno-derivative **2** (Scheme 3). In this case, the reaction sequence started from *trans*-hydroxymesylate **9** with a cyclization reaction with *t*-BuOK in CH_3CN to produce highly reactive vinyl epoxide **10α**, which was treated *in situ* with glycosyl acceptor **15**. Here again, the glycosylation step proved to be very efficient after only 30 minutes at room temperature,

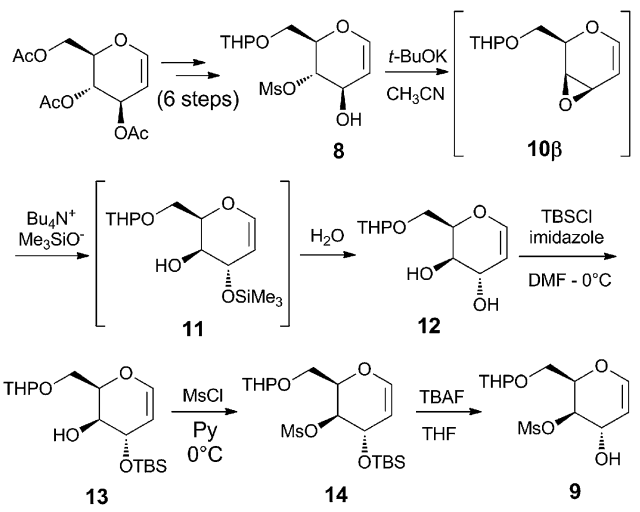

Scheme 2 Synthesis of THP-protected *trans*-hydroxymesylates **8** and **9** from tri-*O*-acetyl-D-glucal.

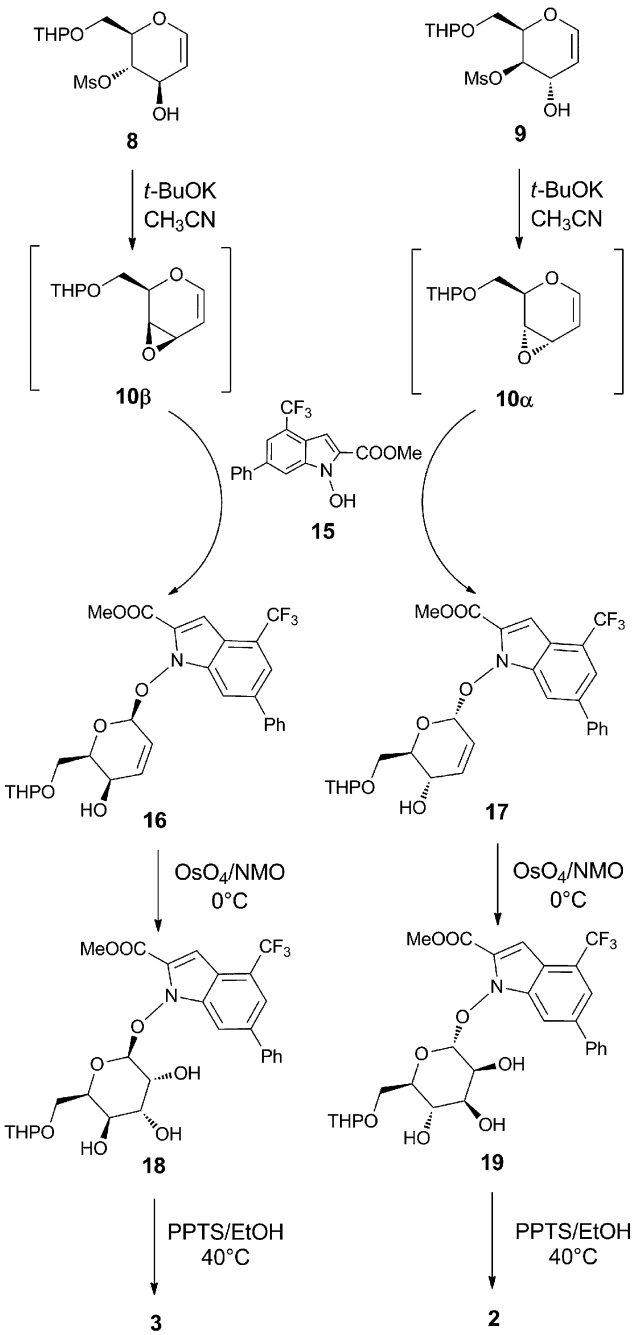

Scheme 3 Synthesis of glycoconjugates **2** and **3** by stereospecific glycosylation of NHI-derivative **15**.

with the production of α-glycoconjugate **17** with a complete 1,4-regio- and α-stereoselectivity (58% yield after purification). Once obtained, the unsaturated α-glycoconjugate **17** was submitted to *cis*-dihydroxylation with OsO_4/NMO and, in this case, the β-stereoselective attack of the electrophile is directed by the allyl substituents at C(4) and C(1), now located on the α-face. Therefore the corresponding β-dihydroxylated derivative **19** was the only stereoisomer obtained (65% yield). The final deprotection of the THP moiety present at C(6) of **19**, carried out in absolute EtOH for 20 h at 40 °C in the presence of PPTS, provided the α-*O*-D-manno-conjugate **2** in 80% yield after recrystallization.

The synthesis of GlcNAc-conjugate **4** (Scheme 4) utilized as the glycosyl donor oxazoline **20**, which was prepared as previously reported.[21] Glycosyl acceptor **15** displayed a low reactivity as the nucleophile with oxazoline **20** and, therefore, we needed to test a wide array of reaction conditions. The best results were obtained by using TMSOTf as the catalyst.[22] This way, the ring opening of oxazoline **20** was realized in anhydrous dichloroethane at 80 °C for 24 h in the presence of molecular sieves 4 Å using 0.5 equiv of TMSOTf and 1.5 equiv of NHI **15** to afford peracetylated Glc-NAc-conjugate **21** in 58% yield after purification. Deacetylation of **21** with MeONa in CH_2Cl_2/MeOH afforded Glc-NAc-conjugate **4** in quantitative yields.

Enzyme inhibition assays

The inhibitory activities of the sugar conjugates **2–4** were measured by standard enzyme kinetic experiments on purified human enzyme isoform *h*LDH5. The K_i values of each compound (Table 1) were measured in NADH-competition experiments as previously described.[12]

All the newly synthesized sugar conjugates (**2–4**) proved to be moderately active in these assays, with K_i values ranging from 68.1 μM with the manno-derivative **3** to 98.4 μM with the amino–glucose-derivative **4**. None of them proved to be more potent than glucose-conjugate **1** (ref. 12) in these *in vitro* assays on the isolated enzyme.

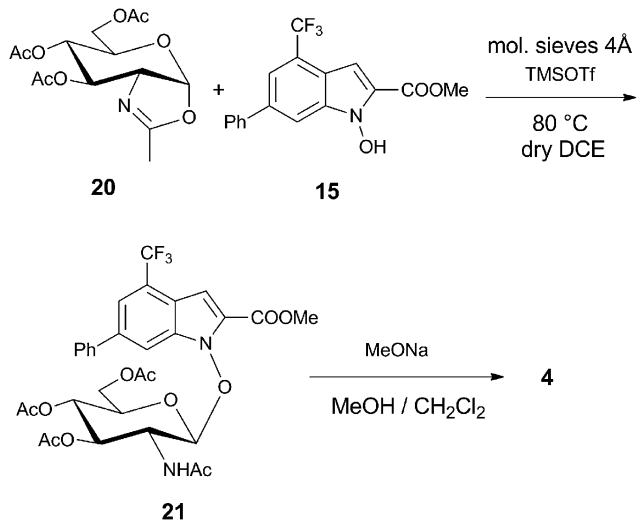

Scheme 4 Synthesis of GlcNAc conjugate **4** *via* the formation of oxazoline **20** and subsequent stereospecific glycosylation of NHI-derivative **15**.

Table 1 *In vitro* kinetic inhibition of sugar conjugates **1–4** against LDH-A[a]

Compound	LDH-A – K_i (μM)
1	37.8 ± 0.9[b]
2	92.4 ± 9.0
3	68.1 ± 17.5
4	98.4 ± 15.6

[a] K_i values were obtained by non-linear regression analysis with GraphPad Prism software (GraphPad, La Jolla, CA) using a second order polynomial regression analysis by applying the mixed-model inhibition fit (mean values ± SD calculated from at least 2 experiments, see Experimental section). [b] From ref. 12.

Molecular modeling

Docking studies followed by molecular dynamic (MD) simulations were carried out to examine the putative modes of interaction of sugar conjugates **2–4** with LDH-A and the results of these studies are shown in Fig. 2.

As highlighted in Fig. 2, all three compounds show a very similar positioning into the LDH-A binding site. In all cases, the C=O portion of the ester group of these compounds forms an H-bond with R169, and the methyl group of the ester establishes lipophilic interactions with the isopropyl side chain of V235. The 4-(trifluoromethyl)indole central scaffold is placed in a cleft mainly delimited by H193, G194, A238, V241, and I242, whereas the 6-phenyl group is directed toward the entrance of the binding site cavity. The sugar moiety is always placed in the NADH-binding pocket but, depending on the type of monosaccharide attached, it shows different H-bonds with the protein. Specifically, the α-mannose ring of **2** (Fig. 2A) forms two H-bonds with the hydroxyl group of T248 through its 2- and 3-hydroxyl groups. The β-gulose ring of **3** (Fig. 2B) shows a slightly different interaction mode with the protein, with a H-bond occurring between its 4-OH group and T248, and a peculiar H-bond that is formed by its 6-OH group and the side chain of N138. Finally, the GlcNAc portion of **4** (Fig. 2C) forms completely different interactions with the enzyme active site, the most important of which seem to be the interaction of the acetamido-group with T248, through its N–H portion, and with R169 through its C=O moiety.

Cellular lactate production inhibition assays

The ability of the glycol-conjugated NHIs **2–4** to inhibit lactate production in cells was evaluated using the same previously reported technique developed for glucose-conjugate **1**,[12] and the results are displayed in Fig. 3.

In testing these glyco-conjugates at 50–200 μM concentrations for their ability to reduce lactate production in HeLa cells following an 8 h incubation, it was found that the α-manno-derivative **2** led to a potent, dose-dependent reduction in lactate production, which is comparable to that obtained with glucose-conjugate **1**, with a remarkable 55% inhibition at the

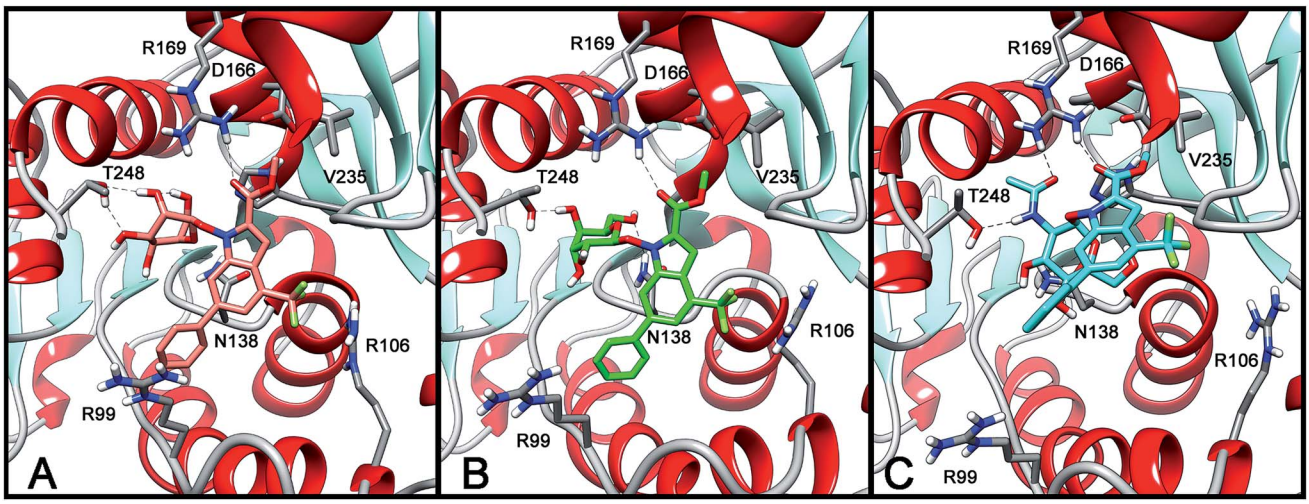

Fig. 2 MD simulation results for the complex of LDH-A with **2** (A), **3** (B), and **4** (C).

lowest concentration used (50 μM). A noticeable dose-dependent activity was also found with β-gulo derivative **3**, although it was lower than those observed with **1** and **2**. On the contrary, GlcNAc-conjugate **4** lacked any significant activity in this assay, and, therefore, was not considered in our subsequent experiments. Under these conditions, a very modest effect is observed with very high concentrations (10 mM) of hexokinase inhibitor 2-deoxyglucose, whereas negligible effects are observed upon incubation with 10 μM of the topoisomerase II inhibitor etoposide, a cytotoxic compound that does not affect glucose metabolism.

Cellular uptake assays

The relative cell uptake levels of glyco-conjugates **2** and **3**, and of reference glucose-conjugate **1**,[12] *versus* their aglycone counterpart NHI-2 (**15**, Scheme 3), and the potential cleavage of the mannose-(**2**) and gulo-portions (**3**) in cell culture, was assessed. A549 cells were treated with 100 μM concentrations of each compound for 4 h. After washing and lysing the cells, the cellular fraction of each compound was assessed by LC-MS and correlated to concentration using calibration standards (Fig. S1, ESI†), and the intracellular concentrations are displayed in Fig. 4.

As we had previously observed with glucose-conjugate **1**,[12] mannose-derivative **2** displays a significantly enhanced cell uptake compared to the aglycone NHI-2. While **1** and **2** had similar levels of cell uptake, the gulose-derivative **3** had slightly lower levels of cell uptake. These results are consistent with those obtained in the cellular lactate production inhibition assays (Fig. 3), where the most potent cellular inhibitors were found to be **1** and **2**, thus positively correlating cellular activity and cell uptake. It is important to note that no cleavage of any of these compounds was observed in either the UV trace or TIC of the resultant lysate samples from 4 h of incubation in A549 cells, so all the effects should be ascribed to the parent compounds.

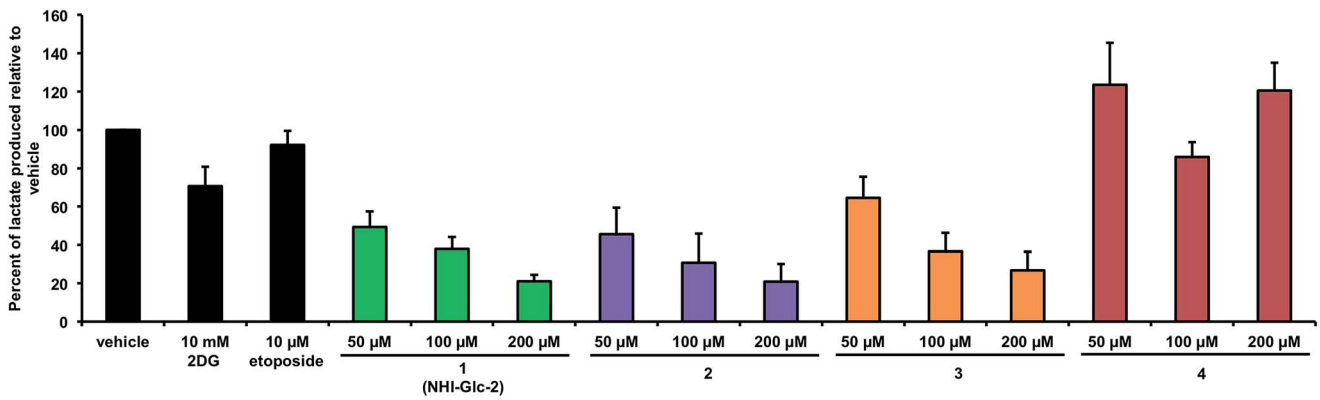

Fig. 3 Lactate production inhibition of glycoconjugates **1–4**. HeLa human cervical carcinoma cells were treated under normoxic conditions with indicated compound concentrations or 1% DMSO vehicle, in DMEM supplemented with 10 mM unlabeled glucose, 1 mM pyruvate, and 4 mM glutamine. Following 8 h incubation, medium aliquots were collected, concentrated, derivatized using MTBSTFA + 1% TBDMCS catalyst, and assessed by GC-MS. Lactate was normalized in each sample using the 1 mM chlorophenylalanine (CPA) internal standard, and lactate relative to vehicle is depicted. Averages from three or more independent experiments are depicted, with error bars depicting standard error ($n \geq 3$).

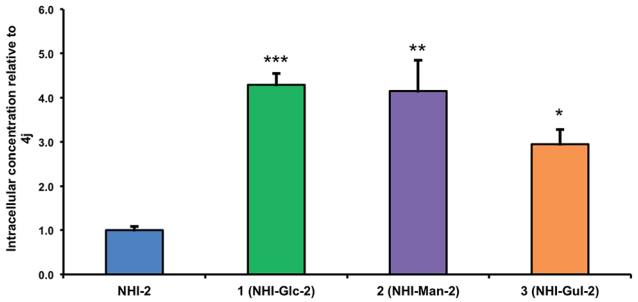

Fig. 4 Results of the intracellular concentration comparison study comparing relative uptake of NHI-2 (**15**) to its three glycoconjugates **1–3**. A549 non-small cell lung carcinoma cells were treated with 100 μM concentrations of each compound for 4 h; cells were then lysed, sonicated in methanol, and assessed for intracellular compound concentration by LC-MS. Triplicate data is shown, with error bars denoting standard error. Statistical analysis was performed using an unpaired Student's *t* test to compare glycoconjugate intracellular concentrations with NHI-2 intracellular concentration, with * denoting $p < 0.05$, ** denoting $p < 0.01$, and *** denoting $p < 0.0005$.

Cancer cell antiproliferative potency assays

After assessing the ability of glycol-conjugates **2** and **3** to penetrate cells and inhibit cellular lactate production, their potency in killing HeLa and A549 cancer cells was evaluated and compared to that of their glucose analogue **1** and of their aglycone NHI-2 (**15**). The growth inhibitory effect of these compounds was evaluated by treating the cancer cells for 72 h with varying concentrations of the compounds, after which cell death was assessed by the Sulforhodamine B (SRB) assay.[23] The antiproliferative potencies are expressed as IC_{50} values (the concentration of compound required to kill 50% of cells, where lower concentrations indicate increased potency) and are presented in Table 2.

Glycoconjugated NHI compounds **1–3** were all more potent in killing cancer cells than their respective aglycone (NHI-2, **15**), in agreement with their increased cell uptake (Fig. 4) and increased cellular lactate production inhibition (Fig. 3) compared to the aglycone. In particular, the newly-synthesized compounds have 3-6-fold (compound **2**) and 2-3-fold (compound **3**) enhanced potencies compared to NHI-2. Finally, the highest potency levels were found with the new mannose-derivative **2**, which is even more potent than glucose-derivative **1**, and shows IC_{50} values of 5.4 μM against HeLa cells and 15.2 μM against A549 cells.

Table 2 Antiproliferative effect (72 h IC_{50} values, μM ± standard error, $n = 3$) of glycoconjugates **1–3** in HeLa and A549 human cancer cell lines[a]

Compound	HeLa (cervical carcinoma)	A549 (NSCLC)
NHI-2 (**15**)	33.4 ± 1.0[b]	44.1 ± 6.2[b]
1	7.2 ± 0.2[c]	17.2 ± 3.0[c]
2	5.4 ± 1.3	15.2 ± 0.7
3	11.8 ± 0.1	24.7 ± 0.9

[a] Three independent experiments were performed under normoxic conditions. Remaining biomass after fixing with 10% trichloroacetic acid was quantified by sulforhodamine B staining. [b] Data from ref. 11. [c] Data from ref. 12.

Conclusions

We have successfully planned and implemented the stereospecific synthesis of three new glycoconjugates (**2–4**), which were intended to extend the chemical class of sugar-conjugates of NHIs. These glycoconjugates were designed to be LDH-A inhibitors with efficient cell uptake. The biological assays in cancer cells displayed a remarkable correlation between the cell uptake, reduction of cellular production of lactate, and inhibition cellular proliferation. Overall, the α-manno-derivative **2** proved to be the most efficient compound in cell-based assays. These results confirm the validity of the dual targeting strategy of the Warburg effect and pave the way to a more expansive exploration of glycoconjugates, both as molecular tools and as potential therapeutic agents that block tumor glycolysis.

Experimental

Materials and methods

All solvents and chemicals were used as purchased without further purification. Chromatographic separations were performed on silica gel columns by flash (Kieselgel 40, 0.040–0.063 mm; Merck) or gravity column (Kieselgel 60, 0.063–0.200 mm; Merck) chromatography. Reactions were followed by thin-layer chromatography (TLC) on Merck aluminum silica gel (60 F_{254}) sheets that were visualized under a UV lamp. Evaporation was performed *in vacuo* (rotating evaporator). Sodium sulfate was always used as the drying agent. Proton (^{1}H) and carbon (^{13}C) NMR spectra were obtained with a Bruker Avance III 400 MHz or Bruker Avance 250 MHz spectrometer using the indicated deuterated solvents. Chemical shifts are given in parts per million (ppm) (δ relative to residual solvent peak for ^{1}H and ^{13}C). Yields refer to isolated and purified products. LC-MS characterization and high-resolution mass spectrometry (HRMS) analysis were performed using a Waters Quattro II quadrupole–hexapole–quadrupole liquid chromatography/mass spectrometry apparatus (Waters, Milford, MA) equipped with an electrospray ionization source. LC separation was achieved using a C18 Waters Xbridge column (2.1 × 20 mm, Waters) at 25 °C using a linear gradient of mobile phases: 95% H_2O, 5% acetonitrile, and 0.1% formic acid (A) and 95% acetonitrile, 5% H_2O, and 0.1% formic acid (B). Solution A was initially passed through the column but decreased linearly to 50% of the mobile phase at 10 minutes and 0% of the mobile phase at 25 minutes. The flow rate was 200 μL min^{-1}, and the injection volume was 10 μL. The ultraviolet (UV) detector was programmed to monitor absorbance at 254 nm, to detect the phenyl ring present in all compounds.

Synthetic procedures

Methyl 1-(((2*S*,5*R*,6*R*)-5-hydroxy-6-(((tetrahydro-2*H*-pyran-2-yl)oxy)methyl)-5,6-dihydro-2*H*-pyran-2-yl)oxy)-6-phenyl-4-(trifluoromethyl)-1*H*-indole-2-carboxylate (16). A solution of *trans*-hydroxymesylate **8** (ref. 20) (0.150 g, 0.488 mmol) in anhydrous CH_3CN (13 mL) was treated with *t*-BuOK (0.060 g, 0.54 mmol, 1.1 equiv) at room temperature and, after the disappearance of the starting material (TLC), with *N*-hydroxyindole derivative **15** (0.180 g, 0.537 mmol, 1.1 equiv) and the resulting reaction mixture was stirred 1 h at the same temperature. After dilution with Et_2O, the organic phase was washed with brine, dried ($MgSO_4$) and concentrated to afford a crude reaction product (0.272 g), which was subjected to flash chromatography. Elution with a 1 : 1 hexane–AcOEt (0.1% Et_3N) mixture afforded pure glycoside **16** (0.206 g, 77% yield) as a liquid. R_f = 0.33 (4 : 6 hexane–AcOEt). ^{1}H NMR (250 MHz; $CDCl_3$) δ 8.13–8.27 (m corresponding to two diastereoisomers, overall 1H; Ar), 7.62–7.96 (m, 3H; Ar), 7.15–7.52 (m, 4H; Ar), 6.23–6.47 (m corresponding to two diastereoisomers, overall 2H; vinyl CH), 5.96–6.05 (m corresponding to two diastereoisomers, overall 1H; anomeric CH), 4.31–4.59 (m corresponding to two diastereoisomers, overall 1H; THP–CHO_2), 3.08–4.15 (m corresponding to two diastereoisomers, overall 6H; CHO & CH_2O), 3.96 (s, 3H; $COOCH_3$), 1.29–1.74 (m corresponding to two diastereoisomers, overall 6H; THP–CH_2).

Methyl 6-phenyl-4-(trifluoromethyl)-1-(((2*S*,3*R*,4*R*,5*R*,6*R*)-3,4,5-trihydroxy-6-(((tetrahydro-2*H*-pyran-2-yl)oxy)methyl)tetrahydro-2*H*-pyran-2-yl)oxy)-1*H*-indole-2-carboxylate (18). A solution of glycoside (**16**) (0.050 g, 0.091 mmol) in an 1 : 1 *t*-BuOH–acetone mixture (0.31 mL) was added to a 50% p/v aqueous solution of *N*-methyl morpholine-*N*-oxide (NMO) (80 μL) and the resulting reaction mixture was treated with 2.5% p/v OsO_4 solution in *t*-BuOH (80 μL) and stirred for 2 h at the same temperature. Dilution with AcOEt and evaporation of the filtered (Celite®) organic solution afforded a crude reaction product (0.092 g), which was subjected to flash chromatography. Elution with a 2 : 8 hexane–AcOEt (0.1% Et_3N) mixture afforded **18** (0.037 g, 70% yield), practically pure as a liquid. R_f = 0.12 (2 : 8 hexane–AcOEt). ^{1}H NMR (250 MHz; $CDCl_3$) δ 8.25–8.31 (m corresponding to two diastereoisomers, overall 1H; Ar), 7.58–7.79 (m, 3H; Ar), 7.34–7.54 (m, 4H; Ar), 5.37–5.49 (m corresponding to two diastereoisomers, overall 1H; anomeric CHO), 5.14–5.25 (m corresponding to two diastereoisomers, overall 1H; THP–CHO_2), 3.90–4.46 (m corresponding to two diastereoisomers, overall 5H; CH_2O and CHO), 3.98 (s, 3H; COOMe), 3.34–3.80 (m corresponding to two diastereoisomers, overall 3H; CH_2O and CHO), 1.40–1.74 (m corresponding to two diastereoisomers, overall 6H; THP–CH_2).

Methyl 6-phenyl-4-(trifluoromethyl)-1-(((2*S*,3*R*,4*R*,5*R*,6*R*)-3,4,5-trihydroxy-6-(hydroxymethyl)tetrahydro-2*H*-pyran-2-yl)-oxy)-1*H*-indole-2-carboxylate (3). PPTS (0.002 g, 0.008 mmol, 0.1 equiv) was added to a solution of 6-OTHP-protected precursor **18** (0.048 g, 0.083 mmol) in absolute EtOH (0.3 mL) and the reaction mixture was carefully stirred 46 h at 40 °C. After dilution with CH_2Cl_2, solid $NaHCO_3$ was added until the solution turned out to be slightly basic. Evaporation of the filtered organic solution afforded a crude solid reaction product which was purified by trituration in hexane, yielding pure **3** (0.031 g, 75% yield) as a white solid. R_f = 0.25 (9 : 1 hexane–acetone). $[\alpha]_D^{20}$: +57.71 (*c* 0.35, CH_3OH). ^{1}H NMR (400 MHz; CD_3OD) δ 8.31–8.36 (m, 1H; Ar), 7.72–7.79 (m, 3H; Ar), 7.45–7.54 (m, 2H; Ar), 7.40 (tt, 1H, J = 7.4, 1.2 Hz; Ar), 7.23 (qd, 1H, J = 1.8, 0.9 Hz; Ar), 5.47 (d, 1H, J = 8.3 Hz; anomeric CHO), 4.11 (t, 1H, J = 3.4 Hz; CHO), 4.03 (dd, 1H, J = 8.3, 3.4 Hz; CHO), 3.98 (s, 3H; COOMe), 3.93 (td, 1H, J = 6.2, 1.1 Hz; CHO), 3.81–3.85 (m, 1H; CHO), 3.79 (dd, 1H, J = 10.8, 4.6 Hz; CH_2O), 3.66 (dd, 1H, J = 10.8, 6.1 Hz; CH_2O). ^{13}C NMR (62.5 MHz; CD_3OD) δ 162.2, 141.2, 140.1, 139.9, 130.1 (2C), 129.8, 129.1, 128.4 (2C), 125.9 (q, J = 271.7 Hz), 124.4 (q, J = 32.3 Hz), 120.1 (q, J = 4.6 Hz), 118.4 (q, J = 1.3 Hz), 115.2, 108.8, 106.7, 75.5, 73.2, 70.4, 68.6, 61.9, 52.4. HRMS: (M + H^+) found 498.1370; $C_{23}H_{23}F_3NO_8$ requires 498.1376.

(2*R*,3*R*,4*S*)-2-(((Tetrahydro-2*H*-pyran-2-yl)oxy)methyl)-3,4-dihydro-2*H*-pyran-3,4-diol (12). A solution of Bu_4NBr (2.94 g, 9.12 mmol, 4.0 equiv) in anhydrous THF (21.0 mL) was treated with Me_3SiOK (1.18 g, 9.12 mmol, 4.0 equiv) and the reaction mixture was stirred at room temperature for 10 min. Filtration through a short (1 cm) Celite column afforded a clear THF solution which was concentrated at reduced pressure (rotary evaporator, final volume about 10 mL) (*Solution B*, containing $Bu_4N^+Me_3SiO^-$, 4.0 equiv). A solution of hydroxymesylate **8** (0.702 g, 2.28 mmol) in anhydrous THF (10.5 mL) was treated with *t*-BuOK (0.282 g, 2.51 mmol, 1.1 equiv) and the reaction mixture was stirred 15 min at room temperature (*Solution A*, containing epoxide **10β**). *Solution B* was added dropwise to *Solution A* and the reaction mixture was stirred 48 h at room temperature. Dilution with Et_2O and evaporation of the washed (brine) organic solution afforded a crude liquid product that was subjected to flash chromatography. Elution with a 3 : 7 hexane–AcOEt (0.1% Et_3N) mixture afforded pure *trans* diol **12** (0.235 g, 45% yield), as a colorless liquid. R_f = 0.13 (3 : 7 hexane–AcOEt). ^{1}H NMR (250 MHz; $CDCl_3$) δ 6.58–6.66 (m corresponding to two diastereoisomers, overall 1H, vinyl CHO), 4.95–5.05 (m corresponding to two diastereoisomers, overall 1H, vinyl CH), 4.64–4.72 (m corresponding to two diastereoisomers, overall 1H, THP–CHO_2), 4.06–4.20 (m corresponding to two diastereoisomers, overall 1H; CHO), 3.77–4.04 (m corresponding to two diastereoisomers, overall 5H CHO and CH_2O), 3.47–3.62 (m corresponding to two diastereoisomers, overall 1H; CHO), 1.69–1.85 (m corresponding to two diastereoisomers, overall 3H, THP–CH_2), 1.48–1.68 (m corresponding to two diastereoisomers, overall 3H; THP–CH_2).

(2*R*,3*S*,4*S*)-4-((*tert*-Butyldimethylsilyl)oxy)-2-(((tetrahydro-2*H*-pyran-2-yl)oxy)methyl)-3,4-dihydro-2*H*-pyran-3-ol (13). Treatment of *trans* diol **12** (0.216 g, 0.939 mmol) in anhydrous DMF (2.5 mL) with imidazole (0.128 g, 1.88 mmol, 2.0 equiv) and TBSCl (0.170 g, 1.13 mmol) afforded, after 18 h stirring at room temperature, a crude liquid product (0.283 g, 88% yield) consisting of mono-silylated **13**, pure as a liquid, which was used in the next step without any purifications. R_f = 0.25 (8 : 2 hexane–AcOEt). ^{1}H NMR (250 MHz; $CDCl_3$) δ 6.49–6.58 (m corresponding to two diastereoisomers, overall 1H; vinyl CHO), 4.81–4.90 (m corresponding to two diastereoisomers, overall 1H; vinyl CH),

4.63–4.71 (m corresponding to two diastereoisomers, overall 1H; THP–CHO_2), 3.95–4.17 (m corresponding to two diastereoisomers, overall 2H; CHO and CH_2O), 3.72–3.94 (m corresponding to two diastereoisomers, overall 4H CHO and CH_2O), 3.43–3.62 (m corresponding to two diastereoisomers, overall 1H, CHO), 1.44–1.86 (m corresponding to two diastereoisomers, overall 6H; THP–CH_2), 0.87 (s, 9H; $(CH_3)_3CSi$), 0.10 (s, 6H; CH_3Si).

(2*R*,3*S*,4*S*)-4-((*tert*-Butyldimethylsilyl)oxy)-2-(((tetrahydro-2*H*-pyran-2-yl)oxy)methyl)-3,4-dihydro-2*H*-pyran-3-yl methanesulfonate (14). Treatment of **13** (0.283 g, 0.82 mmol) in anhydrous pyridine (2.5 mL) with MsCl (0.13 mL, 1.6 mmol, 2.0 equiv) was stirred at 0 °C for 18 h. After concentration under vacuum, the crude product was subjected to flash chromatography. Elution with a 8 : 2 hexane–AcOEt (0.1% Et_3N) mixture afforded pure mesylate derivative **14** (0.254 g, 71% yield) as a yellow liquid. R_f = 0.19 (8 : 2 hexane–AcOEt). ^{1}H NMR (250 MHz; $CDCl_3$) δ 6.45–6.54 (m corresponding to two diastereoisomers, overall 1H; vinyl CHO), 4.82–4.91 (m corresponding to two diastereoisomers, overall 1H; vinyl CH), 4.58–4.76 (m corresponding to two diastereoisomers, overall 2H; CHOMs + THP–CHO_2), 4.22–4.34 (m corresponding to two diastereoisomers, overall 1H; CHO), 4.15–4.21 (m corresponding to two diastereoisomers, overall 1H; CHO), 3.81–4.02 (m corresponding to two diastereoisomers, overall 2H; CH_2O), 3.57–3.80 (m corresponding to two diastereoisomers, overall 1H; CHO), 3.43–3.56 (m corresponding to two diastereoisomers, overall 1H; CHO), 3.04–3.10 (m corresponding to two diastereoisomers, overall 3H; CH_3SO_2), 1.66–1.89 (m corresponding to two diastereoisomers, overall 2H; THP–CH_2), 1.44–1.62 (m corresponding to two diastereoisomers, overall 4H; THP–CH_2), 0.83–0.92 (m corresponding to two diastereoisomers, overall 9H; $(CH_3)_3CSi$), 0.09–0.16 (m corresponding to two diastereoisomers, overall 6H; CH_3Si).

(2*R*,3*R*,4*S*)-4-Hydroxy-2-(((tetrahydro-2*H*-pyran-2-yl)oxy)methyl)-3,4-dihydro-2*H*-pyran-3-yl methanesulfonate (9). Treatment of **14** (0.249 g, 0.589 mmol) in anhydrous THF (20 mL) with 1 M TBAF in THF (0.59 mL, 0.59 mmol) at 0 °C for 20 min. After dilution with Et_2O, evaporation of the washed (brine) and dried ($MgSO_4$) organic solution afforded a crude product, which was subjected to flash chromatography (1 : 1 hexane–AcOEt) to produce pure *trans*-hydroxymesylate **9** (0.122 g, 67% yield) as a yellow liquid. R_f = 0.19 (1 : 1 hexane–AcOEt). ^{1}H NMR (250 MHz; $CDCl_3$) δ 6.53–6.61 (m corresponding to two diastereoisomers, overall 1H; vinyl CHO), 4.93–5.04 (m corresponding to two diastereoisomers, overall 1H; vinyl CH), 4.72–4.87 (m corresponding to two diastereoisomers, overall 1H; THP–CHO_2), 4.59–4.68 (m corresponding to two diastereoisomers, overall 1H; CHOMs), 4.18–4.30 (m corresponding to two diastereoisomers, overall 2H; CH_2O), 3.43–4.05 (m corresponding to two diastereoisomers, overall 4H CHO & CH_2O), 3.04–3.13 (m corresponding to two diastereoisomers, overall 3H; CH_3SO_2), 1.36–1.90 (m corresponding to two diastereoisomers, overall 6H; THP–CH_2).

Methyl 1-(((2*R*,5*S*,6*R*)-5-hydroxy-6-(((tetrahydro-2*H*-pyran-2-yl)oxy)methyl)-5,6-dihydro-2*H*-pyran-2-yl)oxy)-6-phenyl-4-(trifluoromethyl)-1*H*-indole-2-carboxylate (17). A solution of *trans* hydroxymesylate **9** (0.150 g, 0.488 mmol) in anhydrous CH_3CN (12.6 mL) was treated with *t*-BuOK (0.060 g, 0.54 mmol, 1.1 equiv) and, after the disappearance of the starting material (TLC), with *N*-hydroxyindole derivative **15** (0.180 g, 0.537 mmol, 1.1 equiv) and the resulting reaction mixture was stirred for 1 h at room temperature. After dilution with Et_2O, the organic phase was washed with brine, dried ($MgSO_4$) and concentrated to afford a crude reaction product, which was subjected to flash chromatography. Elution with a 1 : 1 hexane–AcOEt (0.1% Et_3N) mixture afforded pure glycoside **17** (0.155 g, 58% yield) as a white solid. R_f = 0.33 (4 : 6 hexane–AcOEt); mp 50–53 °C; ^{1}H NMR (250 MHz; $CDCl_3$) δ 7.77–7.89 (m corresponding to two diastereoisomers, overall 1H; Ar), 7.59–7.76 (m corresponding to two diastereoisomers, overall 3H; Ar), 7.34–7.56 (m corresponding to two diastereoisomers, overall 3H; Ar), 7.27–7.33 (m corresponding to two diastereoisomers, overall 1H; Ar), 6.12–6.36 (m corresponding to two diastereoisomers, overall 2H, vinyl CH), 5.78–5.89 (m corresponding to two diastereoisomers, overall 1H; anomeric CHO), 3.26–4.53 (m corresponding to two diastereoisomers, overall 7H; CH_2O and CHO), 3.94 (s, 3H; COOMe), 1.28–1.86 (m corresponding to two diastereoisomers, overall 6H; THP–CH_2).

Methyl 6-phenyl-4-(trifluoromethyl)-1-(((2*R*,3*S*,4*S*,5*S*,6*R*)-3,4,5-trihydroxy-6-(((tetrahydro-2*H*-pyran-2-yl)oxy)methyl)tetrahydro-2*H*-pyran-2-yl)oxy)-1*H*-indole-2-carboxylate (19). A solution of **17** (0.040 g, 0.073 mmol) in an 1 : 1 *t*-BuOH–acetone mixture (0.25 mL) was added to 50% p/v aqueous solution of *N*-methyl morpholine-*N*-oxide (NMO) (60 μL) and the resulting reaction mixture was treated with 2.5% p/v OsO_4 solution in *t*-BuOH (60 μL) and stirred for 8 h at room temperature. Dilution with AcOEt and evaporation of the filtered (Celite®) organic solution afforded a crude reaction product which was purified by flash chromatography. Elution with a 2 : 8 hexane–AcOEt (0.1% Et_3N) mixture afforded pure α-mannopyranoside **19** (0.028 g, 65% yield) as a white solid. R_f = 0.17 (2 : 8 hexane–AcOEt). ^{1}H NMR (250 MHz; $CDCl_3$) δ 7.76–7.88 (m corresponding to two diastereoisomers, overall 1H; Ar), 7.55–7.72 (m corresponding to two diastereoisomers, overall 3H; Ar), 7.32–7.50 (m corresponding to two diastereoisomers, overall 4H; Ar), 5.66–5.71 (m corresponding to two diastereoisomers, overall 1H; anomeric CHO), 4.66–4.77 (m corresponding to two diastereoisomers, overall 1H; THP–CHO_2), 4.30–4.47 (m corresponding to two diastereoisomers, overall 2H; CHO), 3.93–4.22 (m corresponding to two diastereoisomers, overall 3H; CHO and CH_2O), 3.90 (s, 3H; COOMe), 3.71–3.86 (m corresponding to two diastereoisomers, overall 2H; CH_2O), 3.29–3.48 (m corresponding to two diastereoisomers, overall 1H; CHO), 1.30–1.71 (m corresponding to two diastereoisomers, overall 6H; THP–CH_2).

Methyl 6-phenyl-4-(trifluoromethyl)-1-(((2*R*,3*S*,4*S*,5*S*,6*R*)-3,4,5-trihydroxy-6-(hydroxymethyl)tetrahydro-2*H*-pyran-2-yl)-oxy)-1*H*-indole-2-carboxylate (2). PPTS (0.018 g, 0.007 mmol, 0.1 equiv) was added to a solution of **19** (0.040 g, 0.068 mmol) in absolute EtOH (1.3 mL) and the reaction mixture was stirred for 20 h at 40 °C. After dilution with CH_2Cl_2, solid $NaHCO_3$ was added until the solution turned out to be slightly basic. Evaporation of the filtered organic solution afforded a crude reaction product, which was purified by trituration with hexane, yielding pure α-*O*-D-mannopyranoside **2** (0.014 g, 83% yield) pure as a

white solid. $R_f = 0.08$ (9 : 1 AcOEt–acetone). $[\alpha]_D^{20}$ +18.14 (*c* 0.95, CH_3OH). ^1H NMR (400 MHz; CD_3OD) δ 8.04 (s, 1H; Ar), 7.75–7.78 (m, 3H; Ar), 7.48–7.53 (m, 2H; Ar), 7.41 (tt, 1H, $J = 7.4$, 1.2 Hz; Ar), 7.25–7.29 (m, 1H; Ar), 5.57 (d, 1H, $J = 1.9$ Hz; anomeric CHO), 4.57–4.63 (m, 1H; CHO), 4.20–4.28 (m, 1H; CHO), 3.96 (s, 3H; COOMe), 3.83–3.89 (m, 4H; CH_2O and CHO). ^{13}C NMR (62.5 MHz; CD_3OD) δ 161.3, 141.1, 140.5, 139.2, 130.2 (2C), 129.3, 129.1, 128.5 (2C), 125.2 (q, $J = 271.0$ Hz), 124.8 (q, $J = 32.9$ Hz), 120.2 (q, $J = 4.9$ Hz), 118.3 (q, $J = 1.7$ Hz), 113.6, 111.2, 106.9, 77.5, 72.4, 70.5, 67.9, 62.6, 52.8. HRMS: (M + H^+) found 498.1366; $C_{23}H_{23}F_3NO_8$ requires 498.1376.

(2*R*,3*S*,4*R*,5*R*,6*S*)-5-Acetamido-2-(acetoxymethyl)-6-((2-(methoxycarbonyl)-6-phenyl-4-(trifluoromethyl)-1*H*-indol-1-yl)oxy)tetrahydro-2*H*-pyran-3,4-diyl diacetate (21). Activated molecular sieves 4 Å (0.215 g), oxazoline **20** (ref. 21) (0.230 g, 0.69 mmol, 1.0 equiv) and *N*-hydroxyindole derivative **15** (0.250 g, 0.75 mmol, 1.1 equiv) were dissolved in 3.5 mL of anhydrous DCE and the obtained mixture was stirred at 80 °C until complete dissolution of the reagents. After cooling to room temperature, TMSOTf (60 μL, 0.34 mmol, 0.5 equiv) was added. The resulting solution was heated again at 80 °C and stirred overnight at the same temperature. Then the mixture was diluted with CH_2Cl_2 and filtered; the filtered solution was neutralized by saturated aqueous $NaHCO_3$ and washed with brine. Evaporation of the washed organic solution afforded a crude product, which was subjected to flash chromatography. Elution with a 9 : 1 $CHCl_3$/acetone mixture yielded pure compound **21** (0.140 g, yield 40%) as a pale yellow solid: mp 222–225 °C. $[\alpha]_D^{20} = +26.9$ (*c* 0.79; $CHCl_3$). $R_f = 0.3$ (9 : 1 $CHCl_3$–acetone). ^1H NMR (400 MHz; $CDCl_3$): δ 8.10 (s, 1H; Ar), 7.74 (s, 1H; Ar), 7.63 (d, 2H, $J = 7.7$ Hz; Ar), 7.36–7.49 (m, 3H; Ar), 7.33 (bs, 1H; Ar), 6.70 (d, 1H, $J = 8.6$ Hz; NH), 5.52 (d, 1H, $J = 9.05$, anomeric CHO), 5.16–5.28 (m, 2H; CH_2OAc), 4.55 (q, 1H, $J = 9.0$ Hz; CHOAc), 4.26 (dd, 1H, $J = 12.4$, 4.7 Hz; CHOAc), 3.98–4.08 (m, 1H; CHO), 3.95 (s, 3H; COOMe), 3.69–3.75 (m, 1H; CHN), 2.07 (s, 3H; CH_3CO), 2.03 (s, 3H; CH_3CO), 2.02 (s, 3H; CH_3CO), 1.77 (s, 3H; CH_3CO). ^{13}C NMR (100 MHz; $CDCl_3$): δ 171.0, 170.6 (2C), 169.4, 161.0, 140.2, 140.0, 139.6, 129.2 (2C), 128.3, 127.4 (2C), 124.3 (q, $J = 272.4$ Hz), 123.8 (q, $J = 33.0$ Hz), 120.0 (q, $J = 4.8$ Hz), 119.03 (q, $J = 4.7$ Hz), 117.4 (q, $J = 2.1$ Hz), 114.3, 108.4, 105.8, 73.6, 72.5, 68.0, 61.8, 52.5, 52.4, 23.3, 20.8, 20.7, 20.4.

Methyl 1-(((2*S*,3*R*,4*R*,5*S*,6*R*)-3-acetamido-4,5-dihydroxy-6-(hydroxymethyl)tetrahydro-2*H*-pyran-2-yl)oxy)-6-phenyl-4-(trifluoromethyl)-1*H*-indole-2-carboxylate (4). Compound **21** (56.5 mg, 0.087 mmol, 1.0 equiv) was dissolved in a 2 : 3 mixture of CH_2Cl_2 and MeOH (4 mL) and cooled at 0 °C. A freshly prepared 0.33 M solution of MeONa/MeOH (0.05 mL) was added to the resulting solution and the reaction mixture was stirred for 4 h at room temperature. The mixture was then neutralized with an acidic Amberlite™ IR 120 H resin The resin was then removed by filtration and repeatedly extracted with methanol. The combined filtrate was concentrated under vacuum to give a crude product, which was recrystallized from MeOH to yield pure glycoside **4** (0.020 g, yield 50%) as a pale yellow solid: mp: 190–194 °C. $[\alpha]_D^{20} = -36.9$ (*c* 0,17; MeOH). $R_f = 0.15$ (9 : 1 AcOEt–MeOH). ^1H NMR (400 MHz; DMSO-d_6): δ 8.15 (s, 1H; Ar), 8.06 (d, $J = 9.0$ Hz, 1H, NH), 7.82–7.91 (m, 3H; Ar), 7.50–7.55 (m, 2H; Ar), 7.44 (t, 1H, $J = 7.3$ Hz; Ar), 7.11 (s, 1H; Ar), 5.18–5.21 (m, 2H, 2 × OH), 5.11 (d, $J = 8.7$ Hz, 1H, anomeric CHO), 4.39 (t, $J = 4.8$ Hz, 1H, OH), 3.92 (s, 3H, COOMe), 3.80 (q, $J = 9.0$ Hz, 1H; CHO), 3.41–3.67 (m, 4H; CH_2O, CHO and CHN), 3.11–3.19 (m, 1H; CHO), 1.94 (s, 3H; CH_3CO); ^{13}C NMR (100 MHz; DMSO-d_6): δ 169.4, 159.4, 139.1, 137.7, 137.5, 129.9, 129.2 (2C), 128.1, 127.4 (2C), 124.7 (q, $J = 271.0$ Hz), 122.4 (q, $J = 32.3$ Hz), 119.4 (q, $J = 4.7$ Hz), 117.2 (q, $J = 2.0$ Hz), 113.7, 106.5, 104.2, 77.0, 73.5, 69.8, 60.8, 54.0, 52.3, 23.2. HRMS: (M + H^+) found 539.1639; $C_{25}H_{26}F_3N_2O_8$ requires 539.1641.

Molecular modeling

The compounds were built using Maestro 9.0 (ref. 24) and was subjected to a conformational search (CS) of 1000 steps, using a water environment model (generalized-Born/surface-area model) by means of Macromodel.[25] The algorithm used was based on the Monte Carlo method with the MMFFs force field and a distance-dependent dielectric constant of 1.0. The ligand was then energy minimized using the conjugated gradient (CG) method until a convergence value of 0.05 kcal (mol^{-1} $Å^{-1}$) was reached, using the same force field and parameters used for the CS. The *h*LDH5 chain was extracted from the minimized average structure of the complex between LDH and 1J obtained by us through molecular dynamic simulations.[10] Automated docking was carried out by means of the GOLD 5.1 program.[26] The "allow early termination" option was deactivated, the remaining GOLD default parameters were used, and the ligand was submitted to 30 genetic algorithm runs by applying the ChemScore fitness function. The best docked conformation was taken into account. The so obtained complexes were energy minimized using AMBER 11.[27] Each complex was placed in a rectangular parallelepiped water box, an explicit solvent model for water (TIP3P) was used, and the complex was solvated with a 10 Å water cap. Chloride ions were added as counterions to neutralize the system. Two steps of minimization were then carried out. In the first stage, we kept the complex fixed with a position restraint of 500 kcal (mol^{-1} $Å^{-2}$) and we solely minimized the positions of the water molecules. In the second stage, we minimized the entire system through 20 000 steps of steepest descent followed by conjugate gradient until a convergence of 0.05 kcal (mol^{-1} $Å^{-1}$) was attained. All the α carbons of the protein were blocked with a harmonic force constant of 10 kcal (mol^{-1} $Å^{-2}$). Ten nanoseconds of MD simulation were then carried out. The time step of the simulations was 2.0 fs with a cutoff of 10 Å for the non-bonded interaction, and SHAKE was employed to keep all bonds involving hydrogen atoms rigid. Constant-volume periodic boundary MD was carried out for 400 ps, during which the temperature was raised from 0 to 300 K. Then 9.6 ns of constant pressure periodic boundary MD was carried out at 300 K using the Langevin thermostat to maintain constant the temperature of our system. General Amber Force Field (GAFF) parameters were assigned to the ligand, while partial charges were calculated using the AM1-BCC method as implemented in the Antechamber suite of AMBER 11. The final structure of the complex was obtained as the average of the last 8 ns of MD

minimized by the CG method until a convergence of 0.05 kcal (mol^{-1} $Å^{-1}$). The average structure was obtained using the ptraj program implemented in AMBER 11.

Biological assays

Enzyme inhibition assay. The compounds were evaluated in enzymatic assays to assess their inhibitory properties against commercially available purified human isoform of lactate dehydrogenase *h*LDH5 (LDH-A_4, Lee Biosolution, Inc.). The reaction of lactate dehydrogenase was conducted using the "forward" direction (pyruvate → lactate) and the kinetic parameters for the substrate (pyruvate) and the cofactor (NADH) were measured by fluorescence (emission wavelength at 460 nm, excitation wavelength at 340 nm), to monitor at 37 °C the rate of conversion of NADH to NAD^+ and, therefore, the progression of the reaction. Such assays were conducted in wells containing 200 μL of a solution comprising the reagents dissolved in 100 mM phosphate buffer at pH 7.4. DMSO stock solution of compounds were prepared (concentration of DMSO did not exceed 4% during the measurements). Assays were performed in 96-well plates and compounds were assayed in the presence of scalar concentrations of NADH. They were added in scalar amounts (concentration range = 15–60 μM) to a reaction mix containing phosphate buffer, 1.4 mM pyruvate and a scalar concentration of NADH (10–150 μM), finally LDH solution was added (0.015 U mL^{-1}). LDH activity was measured by recording the decrease in NADH fluorescence using Victor X3 Microplates Reader (PerkinElmer®).

Assessment of lactate production by GC-MS. This assay was performed under normoxic conditions as previously described[12] Briefly, confluent HeLa cervical carcinoma cells (ATCC, Manassas, VA) in a 96 well plate were treated with compound or vehicle control (1% DMSO final concentration in all samples) in DMEM minus phenol red + 10% dialyzed FBS + 1% Penstrep, supplemented with 10 mM glucose, 1 mM sodium pyruvate and 4 mM glutamine, in a final volume of 125 μL per well. Immediately following compound addition, plates were incubated for 4 or 8 h at 37 °C in a 95% air/5% CO_2 atmosphere. Duplicate wells were prepared for each treatment. Following treatment, medium was collected, and 100 μL were added to 2 μL 50 mM chlorophenylalanine (CPA; internal standard for GC-MS analysis). Samples were concentrated, derivatized by a four-hour incubation with MTBSTFA + 1% TBDMCS (Thermo Scientific, Walthman, MA) in acetonitrile at 85 °C, and immediately analyzed using GC-MS (Agilent 6890N GC/5973 MS, equipped with an Agilent DB-5 capillary column, 30 M × 320 μM × 0.25 μM, model number J&W 123-5032, Agilent Technologies, Santa Clara, CA) and an electron impact ionization source. One microliter of each sample was injected using an automated injector, and a solvent delay of 8.20 minutes was implemented. The initial oven temperature was 120 °C, held for 5 minutes; then the temperature was increased at a rate of 10 °C min^{-1} until a temperature of 250 °C was reached. Temperature was then increased by 40 °C min^{-1} until a final temperature of 310 °C was reached. Total run time per sample was 22.5 min.

Compounds were identified using AMDIS Chromatogram software (Amdis, freeware available from amdis.net) and programmed WIST and Niley commercial libraries. The integration area of lactate in each sample was divided by the integration area of CPA in the same sample to achieve a lactate/internal standard ratio. The ratios were averaged for duplicates, and percent lactate production over vehicle was calculated for each independent experiment. The mean lactate production/vehicle was then averaged between three or more independent experiments.

Intracellular concentration assessment. Assessment of intracellular concentration was performed as described previously.[12] A549 human non-small cell lung carcinoma cells (ATCC, Manassas, VA) were grown in T25 cell culture flasks prior to being treated with 100 μM compound or vehicle control (prepared in DMSO) in 5 mL total volume (0.2% final concentration DMSO in all treatments). At each time point, cells were rapidly collected by scraping, washed twice with sterile PBS, 37 °C, and disrupted by sonication in methanol, −80 °C, using an XL-2000 Misonix sonicator (Qsonica, Newton, CT). After a 30 minute incubation at 4 °C to facilitate precipitation of proteins, the sonicates were centrifuged, and a portion of the supernatant was analyzed using the protocol described above. Data analysis was performed using MassLynx spectrometry software (Waters).

These LC-MS parameters allowed for the clear resolution of compound **1** (elution time: 12.4 minutes in the UV trace, 12.6 minutes in the TIC), compound **2** (elution time: 12.7 minutes in the UV trace, 12.9 minutes in the TIC), compound **3** (elution time: 12.9 minutes in the UV trace, 13.1 minutes in the TIC), and **15** (elution time: 15.8 minutes in the UV trace; 16.0 minutes in the TIC). The UV traces of vehicle-treated sonicates from both the start and end of the experiment time course contained no peaks in this range. Calibration curves of **15** and glycoconjugates **1**, **2**, and **3** demonstrated a linear relationship between concentration and UV trace integration area, so a linear equation was generated for each compound to convert integration area to concentration.

Cell proliferation assay. Determination of cellular IC_{50} values was performed under normoxic conditions as described previously.[12] Briefly, HeLa and A549 cells, grown in RPMI 1640 medium supplemented with 10% FBS and 1% Penicillin/Streptomycin, were added at a density of 5000 cells per well to 96 well plates to which 31.6 nM–200 μM compound in DMSO was already added (1% final concentration DMSO in all wells; triplicate wells at the same concentration per repetition). Plates were incubated at 37 °C in a 95% air/5% CO_2 atmosphere for 72 h. Medium was removed and cells were fixed by the addition of 50 μL 10% trichloroacetic acid in water, 4 °C, to each well. Plates were incubated at 4 °C for at least one hour, and the sulforhodamine B colorimetric assay[23] was performed to assess remaining biomass in each well. Cells treated with 1% DMSO were used as the 100% live control for biomass, and wells incubated with medium alone were used as the baseline zero biomass control. IC_{50} values were calculated using SoftMax Pro software (Molecular Devices, Sunnyvale, CA).

Acknowledgements

Support from the National Institutes of Health (R01GM098453) is gratefully acknowledged. ECC is supported by an NCI F30 Ruth L. Kirschstein National Research Service Award (1F30CA168323).

Notes and references

1 O. Warburg, *Science*, 1956, **124**, 269–270.
2 P. F. Oliveira, A. D. Martins, A. C. Moreira, C. Y. Cheng and M. G. Alves, *Med. Res. Rev.*, 2015, **35**, 126–151.
3 C. Granchi and F. Minutolo, *ChemMedChem*, 2012, **7**, 1318–1350.
4 C. Granchi, D. Fancelli and F. Minutolo, *Bioorg. Med. Chem. Lett.*, 2014, **24**, 4915–4925.
5 (*a*) V. R. Fantin, J. St-Pierre and P. Leder, *Cancer Cell*, 2006, **9**, 425–434; (*b*) H. Xie, J. Hanai, J. G. Ren, L. Kats, K. Burgess, P. Bhargava, S. Signoretti, J. Billiard, K. J. Duffy, A. Grant, X. Wang, P. K. Lorkiewicz, S. Schatzman, M. Bousamra II, A. N. Lane, R. M. Higashi, T. W. Fan, P. P. Pandolfi, V. P. Sukhatme and P. Seth, *Cell Metab.*, 2014, **19**, 795–809.
6 T. Kanno, K. Sudo, M. Maekawa, Y. Nishimura, M. Ukita and K. Fukutake, *Clin. Chim. Acta*, 1988, **173**, 89–98.
7 C. Granchi, S. Bertini, M. Macchia and F. Minutolo, *Curr. Med. Chem.*, 2010, **17**, 672–697.
8 C. Granchi, I. Paterni, R. Rani and F. Minutolo, *Future Med. Chem.*, 2013, **5**, 1967–1991.
9 E. C. Calvaresi and P. J. Hergenrother, *Chem. Sci.*, 2013, **4**, 2319–2333.
10 C. Granchi, S. Roy, C. Giacomelli, M. Macchia, T. Tuccinardi, A. Martinelli, M. Lanza, L. Betti, G. Giannaccini, A. Lucacchini, N. Funel, L. G. León, E. Giovannetti, G. J. Peters, R. Palchaudhuri, E. C. Calvaresi, P. J. Hergenrother and F. Minutolo, *J. Med. Chem.*, 2011, **54**, 1599–1612.
11 C. Granchi, E. C. Calvaresi, T. Tuccinardi, I. Paterni, M. Macchia, A. Martinelli, P. J. Hergenrother and F. Minutolo, *Org. Biomol. Chem.*, 2013, **11**, 6588–6596.
12 E. C. Calvaresi, C. Granchi, T. Tuccinardi, V. Di Bussolo, R. W. Huigens, H. Y. Lee, R. Palchaudhuri, M. Macchia, A. Martinelli, F. Minutolo and P. J. Hergenrother, *ChemBioChem*, 2013, **14**, 2263–2267.
13 J. E. Barnett, G. D. Holman and K. A. Munday, *Biochem. J.*, 1973, **131**, 211–221.
14 H. Lodish, A. Berk, S. L. Zipursky, P. Matsudaira, D. Baltimore and J. Darnell, in *Molecular Cell Biology*, ed. W. H. Freeman, New York, 4th edn, 2000, http://www.ncbi.nlm.nih.gov/books/NBK21669/.
15 Z. Ma and K. Vosseller, *Amino Acids*, 2013, **45**, 719–733.
16 Z. Ma and K. Vosseller, *J. Biol. Chem.*, 2014, **289**, 34457–34465.
17 V. Di Bussolo, M. Caselli, M. Pineschi and P. Crotti, *Org. Lett.*, 2002, **4**, 3695–3698.
18 V. Di Bussolo, M. Caselli, M. Pineschi and P. Crotti, *Org. Lett.*, 2003, **5**, 2173–2176.
19 V. Di Bussolo, M. Caselli, M. R. Romano, M. Pineschi and P. Crotti, *J. Org. Chem.*, 2004, **69**, 7383–7386.
20 V. Di Bussolo, L. Checchia, M. R. Romano, M. Pineschi and P. Crotti, *Org. Lett.*, 2008, **10**, 2493–2496.
21 S. Nakabayashi, C. D. Warren and R. W. Jeanlozs, *Carbohydr. Res.*, 1986, **150**, C7–C10.
22 K. Křenek, P. Šimon, L. Weignerová, B. Fliedrová, M. Kuzma and V. Křen, *Beilstein J. Org. Chem.*, 2012, **8**, 428–432.
23 V. Vichai and K. Kirtikara, *Nat. Protoc.*, 2006, **1**, 1112–1116.
24 *Maestro, version 9.0*, Schrödinger Inc, Portland, OR, 2009.
25 *Macromodel ver. 9.7*, Schrödinger Inc, Portland, OR, 2009.
26 M. L. Verdonk, J. C. Cole, M. J. Hartshorn, C. W. Murray and R. D. Taylor, *Proteins*, 2003, **52**, 609–623.
27 D. A. Case, T. A. Darden, T. E. Cheatham III, C. L. Simmerling, J. Wang, R. E. Duke, R. Luo, R. C. Walker, W. Zhang, K. M. Merz, B. Roberts, B. Wang, S. Hayik, A. Roitberg, G. Seabra, I. Kolossváry, K. F. Wong, F. Paesani, J. Vanicek, J. Liu, X. Wu, S. R. Brozell, T. Steinbrecher, H. Gohlke, Q. Cai, X. Ye, J. Wang, M.-J. Hsieh, G. Cui, D. R. Roe, D. H. Mathews, M. G. Seetin, C. Sagui, V. Babin, T. Luchko, S. Gusarov, A. Kovalenko and P. A. Kollman, *AMBER 11*, University of California, San Francisco, CA, 2010.

